

# SOLIDIFICATION BEHAVIOUR AND MICROSTRUCTURE OF A360-SiC<sub>p</sub> CAST COMPOSITES

**P. Bassani\*, B. Previtali\*\*, A. Tuissi\*, M. Vedani\*\*, G. Vimercati\*\*, S. Arnaboldi\*\***

**\* CNR IENI, Lecco, Italy**

**\*\* Politecnico di Milano, Milan, Italy**

## **Abstract**

In the present investigation, the solidification microstructure of Al based composites was studied. The materials investigated were a commercial A360 aluminium alloy and the corresponding composites reinforced with 10 and 20 vol.% SiC particles. The materials were cast under different conditions for a first set of laboratory tests, aimed at studying the solidification behaviour and the related microstructures. The reinforcement distribution in the cast composites revealed to be governed by the pushing action exerted by the matrix solidification front during casting, giving rise to clustering effects of the SiC at dendrite boundaries, especially in sand castings. Copper mould castings, experiencing reasonably high cooling rates during solidification, showed a very fine microstructure within which the segregational effects of the reinforcement was of limited relevance. SiC particles also revealed to be a site for heterogeneous nucleation of coarse Si crystals in the composites

## **Riassunto**

Nel presente studio si sono volute analizzare le microstrutture di solidificazione di materiali compositi a matrice in lega di alluminio. I materiali utilizzati sono stati una lega commerciale A360 di alluminio e i corrispondenti compositi rinforzati rispettivamente con il 10% e il 20% in volume di particelle di SiC. I materiali sono stati colati in differenti condizioni per una prima serie di analisi di laboratorio, con lo scopo di studiare il comportamento di solidificazione e le relative microstrutture. La distribuzione del rinforzo nei getti in composito si è rilevata essere governata da fenomeni di “pushing” esercitati dal fronte di solidificazione durante la colata, generando, in particolar modo nei getti in sabbia, fenomeni di segregazione del SiC ai bordi delle dendriti. Colate in lingottiera in rame, che come noto garantiscono elevate velocità di raffreddamento in fase di solidificazione, hanno permesso di ottenere microstrutture molto fini, con fenomeni di segregazione del rinforzo di limitata rilevanza. Inoltre nei compositi le particelle di SiC si sono rilevate essere in grado di promuovere una nucleazione eterogenea di grossolani cristalli di silicio primario.

## INTRODUCTION

Metal matrix composites (MMCs) are a promising group of materials, produced by combining a metallic alloy matrix, usually an aluminium alloy, with a hard and stiff ceramic reinforcement. Their properties can be tailored by a proper selection of matrix properties and by changing the composition, shape, size and volume fraction of the reinforcing phase. Interesting application fields exist in the automotive and aerospace sectors, electronic packaging as well as in sport equipments [1,2].

Discontinuously reinforced MMCs, such as particulate reinforced aluminium alloys, offer the additional advantage of being amenable to a large part of the conventional metalworking techniques usually adopted for the corresponding unreinforced alloys. However, due to the effects of the abrasive ceramic particles in the composite, machining undoubtedly remains one of the less attractive routes for obtaining complex parts. For this reason, cast composite parts, whose final shape is directly obtained by solidification, are considered of strategically importance for a rapid uptake of

MMCs in advanced industrial applications [3].

The solidification behaviour of particulate reinforced MMCs is strongly influenced by the interaction of the solid reinforcement phase with the solidification front. Depending on physical properties of ceramic reinforcement and liquid matrix, and on solidification conditions (e.g.: temperature gradient and solidification rate), particle pushing ahead of the solidification front rather than reinforcement engulfment in the solidified metal matrix can occur. These possibilities in turn significantly affect the degree of reinforcement distribution of the cast composite since, when the particles are rejected in the liquid phase, they will concentrate in the interdendritic regions of the structure, leading to harmful segregation effects [1,4-8].

From a technological perspective, there are other peculiar aspects that deserve special attention when comparing the foundry procedures of Al based MMCs with respect to those of the unreinforced alloys. Melting is usually performed in conventional furnaces based on gas combustion, resistance or induction heating. However, particle settling must be prevented by periodical stirring of the melt. Temperature should be strictly controlled at any time in order to avoid unwanted reaction between SiC and Al that would occur on overheating [9-12]. Skimming as well as degassing to increase melt cleanliness are not usually accomplished in MMC melts due to the tendency of reinforcement accumulation at melt surface that would result. Therefore, the starting ingots and all the equipments to be used in contact with the composite melt have to be carefully cleaned and devoid of humidity.

## MATERIALS AND EXPERIMENTAL PROCEDURES

The materials studied in the present investigations are an A360 alloy and two composites obtained by the addition of 10 and 20% (nominal content) of SiC particles. The composition of the materials investigated is listed in Table I. The materials were provided in the form of commercial foundry ingots weighting about 12 kg.

A first set of castings was produced by a laboratory vacuum induction melting furnace (Balzers VSG 10) equipped with a ZrO<sub>2</sub> (65%)/SiO<sub>2</sub> (35%) crucible. For electromagnetic coupling, the melting crucible was inserted in an external graphite crucible (Figure 1). Melting operations were conducted

under controlled Argon atmosphere at a pressure of 650 mbar and the materials were cast in a square-section (70x70 mm) water-cooled copper mould. A thermocouple was positioned at the centre of the mould in order to record the ingot temperature during solidification and cooling. To evaluate the effectiveness of electromagnetic stirring of the liquid Al alloy and the suspension of the solid SiC particles, no mechanical stirring of the melt was performed.

A second set of castings was then produced with an industrial gas furnace at a foundry plant. For this case, the melt was periodically stirred both during melting and just before pouring to prevent particle settling. For a set of castings, modification of the alloy was performed by using Na-based additives, according to conventional foundry practice. The molten alloy and composites were then poured in dry sand moulds having two different shapes. Simple cylindrical shaped castings of 50 mm in diameter and 80 mm in height were produced as samples for the laboratory analyses. Also in these circumstances, the temperature was measured by a thermocouple

TABLE 1. CHEMICAL COMPOSITION (MASS %) OF THE A360 ALLOY AND OF THE MATRIX OF THE COMPOSITES INVESTIGATED

Alloy	Si	Fe	Cu	Mn	Mg	Cr	Zn	Ti	Ni	Sr	Al
A360	9,23	0,49	0,079	0,30	0,34	0,017	0,063	0,03	0,001	-	bal.
A360-10%SiC	10,8	0,90	0,004	0,76	0,63	0,002	0,005	0,09	0,005	0,010	bal.
A360-20%SiC	9,94	0,89	0,007	0,62	0,63	-	0,013	0,08	-	-	bal.

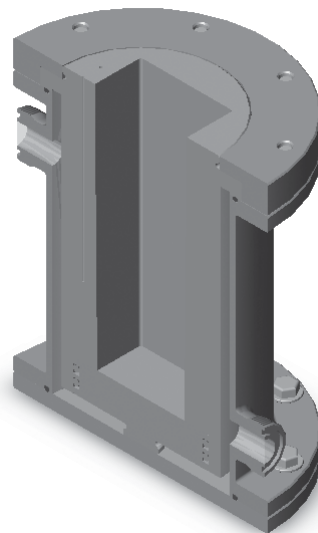
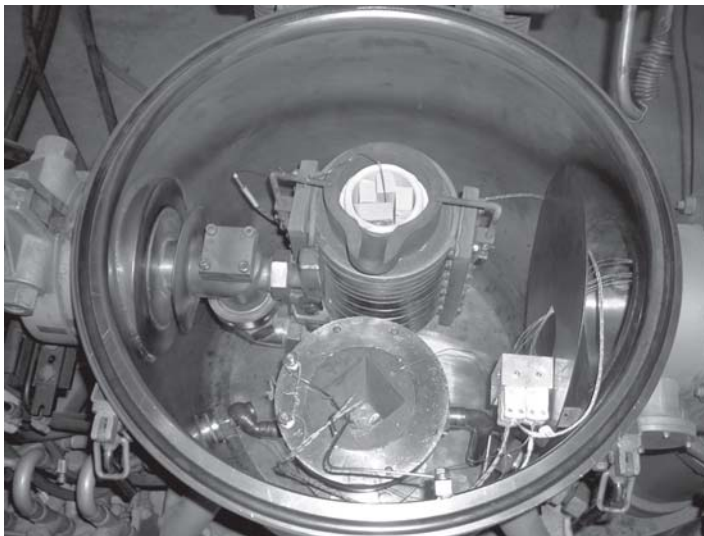


Fig. 1: Experimental set-up for laboratory scale castings. Insight of the vacuum chamber (a) and schematic section of the water-cooled copper mould (b).

placed at cylinder axis. In addition, a series of much larger castings, weighting about 10 kg, were produced as depicted in Figure 2. Detail on the properties of these latter castings will be presented in a future paper.

Samples cut from the sectioned castings were then investigated for microstructural analyses to study the effects of the different solidification conditions and of the different amount of reinforcement on the structure

of the A360 alloy. Optical and scanning electron microscopy (SEM) as well as hardness and microhardness measurements were adopted for the microstructural analyses presented in this paper.

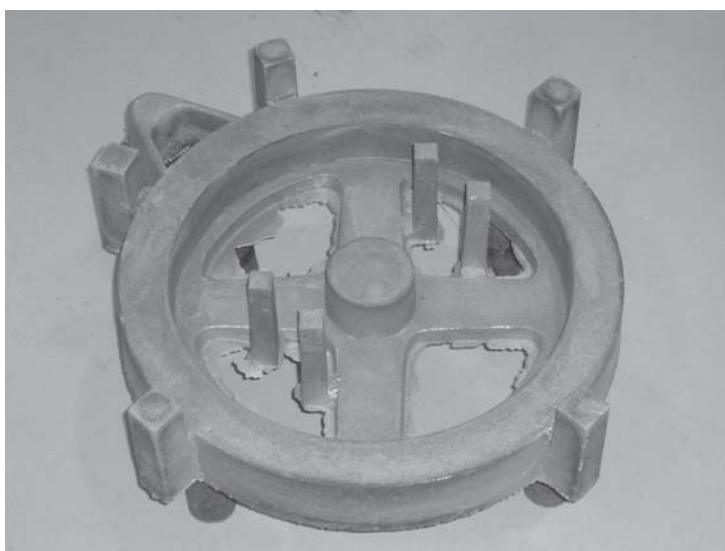


Fig. 2: MMC castings produced according to foundry practice. Pouring of the composite melt in the sand mould (a) and MMC complex-shape casting (b).

## RESULTS AND DISCUSSION

### COOLING CURVES AND COOLING RATES

In Figures 3 and 4 the cooling curves of the materials investigated are reported for water-cooled copper-mould castings and cylindrical sand castings, respectively.

An estimation of the cooling rates experienced by the composites on solidification was obtained by calculating the first derivative of the temperature-time curves. The cooling rate curves are also reported in figures 3 and 4.

Interpretation of the cooling curves and their derivatives can be obtained by knowledge of the equilibrium solidification sequence and by other published works [13,14]. It is well established that the initially high cooling rate corresponds to liquid cooling, solidification onset is marked by the nucleation of primary  $\alpha$ -Al phase from the liquid, resulting in a large decrease of the solidification rate with its main thermal effects corresponding to the first downward peak in the cooling rate curves. After a short period, the Al-Mg<sub>2</sub>Si-Si ternary eutectic solidification occurs under quasi-isothermal conditions, resulting in a plateau of the cooling curve profiles. As a rough estimation, from the recorded cooling curves, it is possible to state that, at the first stages of solidification, the cooling rate in the water cooled copper mould was of the order of 200°C/min whereas the cooling rate in the sand castings was of about 25°C/min. Completion of cooling was reached after about 60 second in water cooled mould, while it took about 10 minutes for sand mould.

Inspection of the cooling curves of the three materials also suggests that the solidification behaviour of the matrix alloy is apparently not affected by the presence of the SiC particles. As expected, the length of the eutectic solidification plateau is a direct function of the amount of alloy poured into the moulds and therefore not strictly constant for the tests performed in this investigation. More accurate considerations would suggest that the solidification time of the eutectic should also be proportional to the amount of matrix alloy (i.e. decreasing with increasing SiC content) [14].

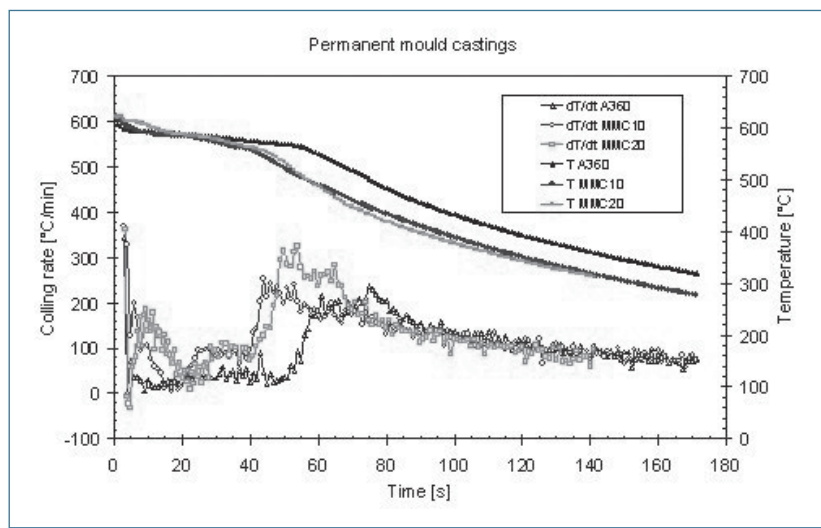


Fig. 3: Cooling curves and cooling rate curves of the copper permanent mould castings.

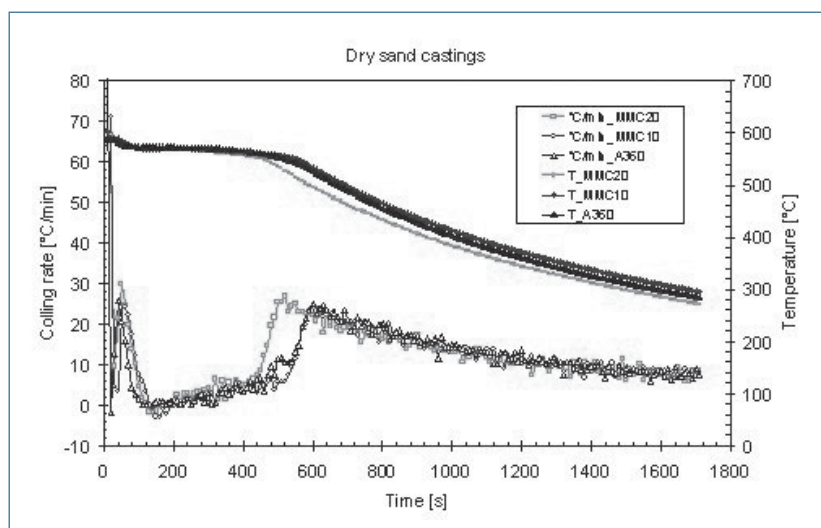


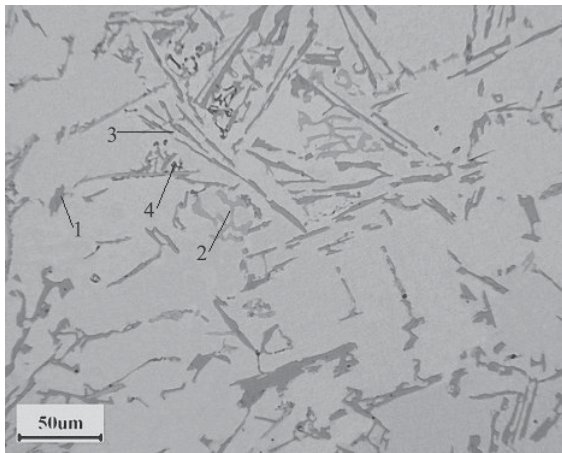
Fig. 4: Cooling curves and cooling rate curves of the cylindrical sand castings.

### MICROSTRUCTURE

Preliminary analyses on the as received composite ingots were carried out to identify the main phases in the unreinforced A360 alloy and in the composite matrices. Irrespective of reinforcement content, the matrix alloy was formed by the  $\alpha$ -Al solid solution and by four types of secondary phases. Electron probe microanalyses were carried out on unetched samples to identify the nature of these constituents. Their chemical compositions were analytically treated to account for the unwanted interaction of the X-ray beam with the matrix surrounding the smallest phases [15]. Si platelets and coarse primary Si crystals, Mg<sub>2</sub>Si, FeMg<sub>3</sub>Si<sub>6</sub>Al<sub>8</sub>, (FeMn)<sub>3</sub>Si<sub>2</sub>Al<sub>15</sub> were identified as the main intermetallics constituting the matrix alloy. These phases could also be easily recognised in optical micrographs due to their contrast in colour and typical shape, as shown in Figure 5a. The composite structure additionally featured the presence of blocky-shaped, roughly equiaxed SiC particles, whose average size was of 6 micrometers, as depicted in Figure 5b.



A)



B)

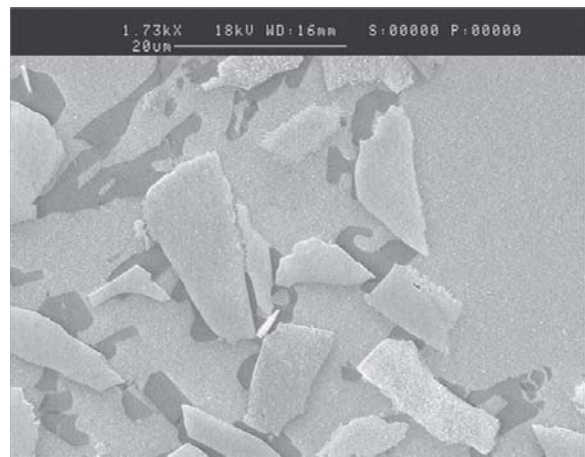
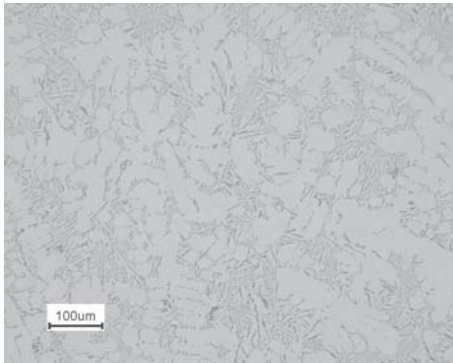
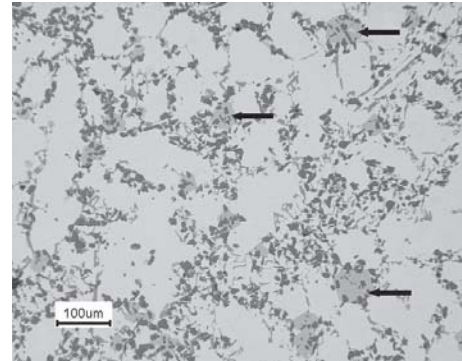


Fig. 5: Representative micrographs of the as received A360 alloy (a) and of the A360-20%SiC composite (b). In figure 5a the labels correspond to the following phases: (1)  $\text{FeMg}_3\text{Si}_6\text{Al}_8$ ; (2)  $(\text{FeMn})_3\text{Si}_2\text{Al}_{15}$ ; (3) Si platelets; (4)  $\text{Mg}_2\text{Si}$ .

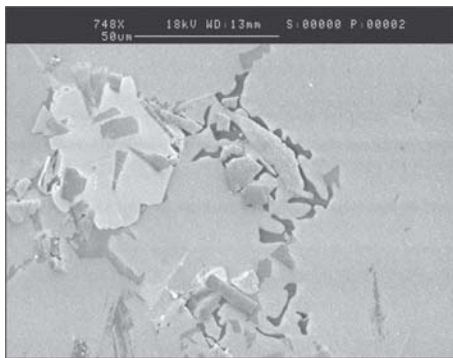
A)



B)



C)



D)

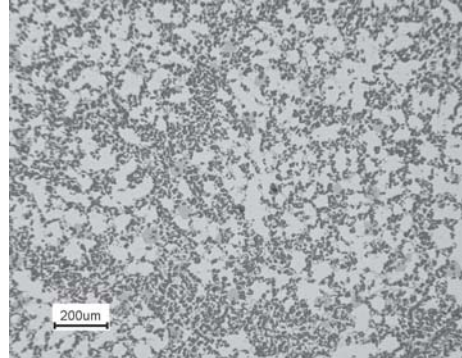
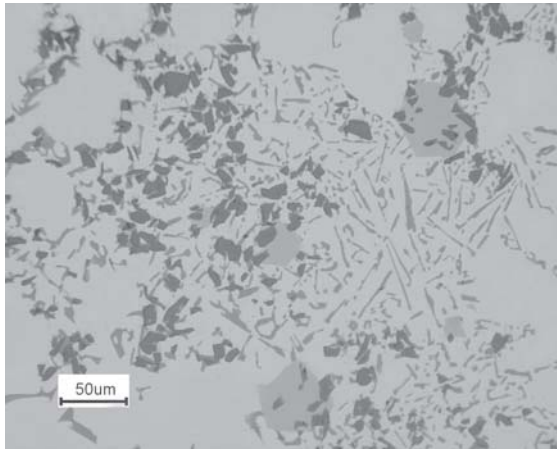


Fig. 6: Micrographs of the unmodified sand cast A360 alloy (a), of the A360-10%SiC composite (b and c) and of the A360-20%SiC composite (d).

Analyses on the cylindrical sand castings showed that the reinforcement distribution was fairly homogeneous, at least on a macroscopic scale. From a microstructural viewpoint, it was noticed that the reinforcement particles were preferably segregated in the interdendritic regions (Figure 6), i.e. SiC was pushed by the growing  $\alpha$ -dendrites and gathered together with the

eutectic constituent at dendrite boundaries. High-magnification views of the structure showed that the SiC particles featured well defined edges and a shape substantially comparable to those detected in the as-received ingots, thus supporting the

A)



B)

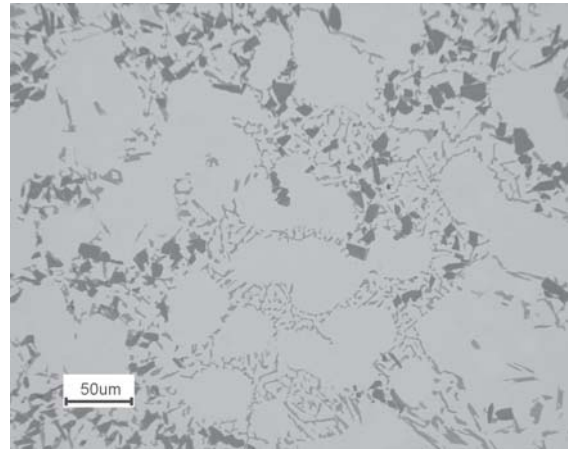


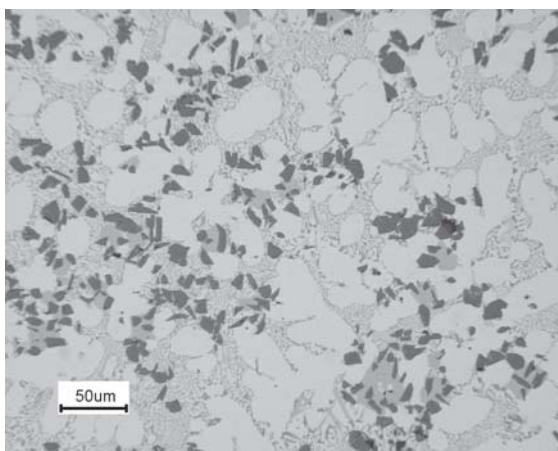
Fig. 7: Comparison of the unmodified (a) and Na-modified (b) structure in the sand cast A360-10%SiC composite.

hypothesis of absence of significant matrix-reinforcement reactions occurring during melting and casting of the materials. In addition, it was observed that coarse Si crystals were distributed in the structure of the composites (arrowed dark grey phases in Figure 6b). From inspection at higher magnification, there was reasonable evidence that these coarse crystals took their origins by heterogeneous nucleation at SiC particles (light phase containing several SiC particles in Figure 6c). Similar conclusions concerning the nucleation of the Si phase at SiC particles were already given in literature for the eutectic Si platelets [2,13,16,17] and for the primary Si crystals [14]. Of particular relevance for the present investigation is the

observation that SiC particles can promote the formation of primary Si crystals even in hypoeutectic alloys such as the A360 alloy matrix. The nucleation role played by SiC is also confirmed by the fact that no primary Si crystals were detected by careful observations of the unreinforced A360 alloy samples (see Figure 6a).

The effect of Na-based modifier in order to change the shape of the Si platelets is depicted in figure 7. It is inferable that the modified eutectic features tiny Si particles whose shape is nearly spherical or at least equiaxed, as opposed to the more elongated shape of the unmodified samples (see also figure 5b). It is well established that this morphology gives improved ductility properties when compared to the unmodified eutectic [14,18,19]. Figure 8 depicts representative micrographs of the water-cooled copper-mould cast composites. As already mentioned, these castings underwent a rapid solidification leading to a much finer grain structure. For this condition, the size of the matrix grains became of the same order of magnitude of the

A)



B)

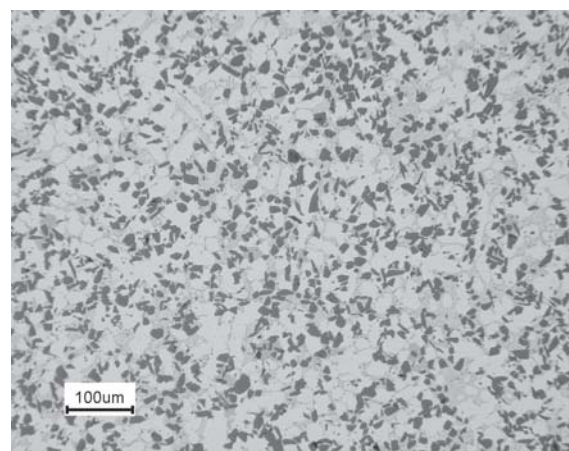


Fig. 8: Optical micrographs of the water-cooled copper mould castings (a) A360-10%SiC composite, (b) A360-20%SiC composite.

reinforcement particles. The tendency toward SiC clustering to dendrite boundaries was thus less evident due to the limited segregation path allowed to the reinforcement. For this reason, the dispersion of reinforcement in the copper mould cast composites was remarkably improved. However, lack of homogeneity was still noted in the A360-10%SiC composite in lower magnification micrographs, where regions of reinforcement free matrix were observed (Figure 8a). This effect was supposed to be related to uneven

reinforcement distribution in the liquid melt before casting.

Finally, it is worth emphasizing that the only casting defects detected consisted of small and isolated microvoids related to shrinkage phenomena, a few tenths of micrometer in size, often located within SiC particle clusters.

### HARDNESS

Table II summarizes the average Vickers hardness values of the materials investigated together with the standard deviation of data.

TABLE II. VICKERS HARDNESS VALUES OF THE MATERIALS INVESTIGATED

Alloy	Copper mould casting	Sand casting	Sand casting (Na modified)
A360	78,6 ± 4,5	63,6 ± 2,6	-
A360-10%SiC	105,6 ± 4,1	97,0 ± 9,1	93,3 ± 8,0
A360-20%SiC	125,3 ± 10,8	107,3 ± 14,9	109,3 ± 11,8

From analysis of the hardness data it can be stated that the largest effect is played by the reinforcement content, leading to a monotonic increase of hardness when increasing the SiC content. As expected, solidification rate also plays a remarkable role, especially in the unreinforced alloy, while the effects of Na-modification revealed to be less defined, being of the same order of the experimental data scatter.

### CONCLUSIONS

From the investigations on the A360-alloy based particulate-reinforced composites, the following conclusions could be drawn.

1. The composites could be satisfactorily cast in different shapes and by different processes, experiencing a large range of cooling rates.
2. Induction melting generally allowed to achieve good homogeneity of the molten alloy due to electromagnetic stirring. This effect also revealed to be suitable to retain a satisfactory dispersion of the reinforcement particles, preventing SiC settling due to difference in density with the matrix alloy.
3. Sand casting were successfully produced by mechanical stirring of the melt. Due to larger dendrite size, the SiC distribution was less homogeneous from a microstructural viewpoint. Only small casting defects related to microshrinkage phenomena were detected in the sand cast samples.

4. In the solidified composites, the SiC particles were generally located at dendrite boundaries due to the pushing action exerted by the solidification front. When the dendrite-branch size became of the same order of magnitude of the particle size (copper moulds), this effects was less relevant. However, local SiC-depleted regions related to uneven reinforcement distribution in the liquid composite were still noticed in the 10%SiC-reinforced composites.
5. The presence of SiC particles also revealed to promote the formation of coarse primary Si crystals in the composite structure.
6. Na-based modification of the eutectic was used during a set of sand casting of the composites. The effectiveness of the Si-platelets modification was demonstrated.

### ACKNOWLEDGEMENT

The present research was performed with the financial support of Fondazione CARIPLO. The authors would also like to acknowledge the skilful contribution of Fonderia Flli Liotti SrL (Verbania, Italy) for their support in preparing the foundry sand castings and Mr. M. Pini for the laboratory copper-mould castings.

## REFERENCES

- [1] Warren H.H., Darrell R.H. Metal matrix composites. *Adv. Mater. Proc.* 2004;2:39-42.
- [2] Surappa M.K. Microstructure evolution during solidification of DRMMCs: state of the art. *J. Mater. Proc. Techn.* 1997;63:325-333.
- [3] Klimowicz T.F. The large scale commercialisation of aluminium-matrix composites. *J. Metals* 1994 ;46(11) :49-53.
- [4] Kim J.K., Rohatgi P.K. The effect of the diffusion of solute between the particle and the interface on the particle pushing phenomena. *Acta Mater.* 1998;46(4):1115-1123.
- [5] Juretzko F.R., Dhindaw B.K., Stefanescu D.M., Sen S., Curreri P.A. Particle engulfment and pushing by solidification interfaces: part I – ground experiments. *Metall Mater Trans* 1998;29A(6):1691-169.
- [6] Mukherjee S., Stefanescu D.M. Liquid convection effects on the pushing-engulfment transition of insoluble particles by a solidifying interface: Part I – analytical calculation of the lift forces. *Metall. Mater. Trans.* 2004;35A(2):613-621.
- [7] Sasikumar R., Kumar M. Redistribution of particles during casting of composite melts: effects of buoyancy and particle pushing. *Acta Metall. Mater.* 1991;39(11):2503-2508.
- [8] Kaptay G. Reduced critical solidification front velocity of particle engulfment due to an interface active solute in the liquid metal. *Metall. Mater. Trans.* 2002;33A:1869-1873.
- [9] Ocelik V., Vreeling J.A., De Hosson J.T. EBSP study of reaction zone in SiC/Al metal matrix composites prepared by laser melt injection. *J. Mater. Sci.* 2001;36:4845-4849.
- [10] Yan M., Fan Z. Review – durability of materials in molten aluminium alloys. *J. Mater. Sci.* 2001;36:285-295.
- [11] Kobashi M., Choh T. The wettability and the reaction for SiC particle/Al alloy system. *J. Mater. Sci.* 1993;28:684-690.
- [12] Howe J.M. Bonding, structure and properties of metal/ceramic interfaces: Part I Chemical bonding, chemical reaction and interfacial structure. *Int. Mater. Rev.* 1993;38(5):233-256.
- [13] Braszczynski J., Zyska A. Analysis of the influence of ceramic particles on the solidification process of metal matrix composites. *Mater. Sci. Engng.* 2000;A278:195-203.
- [14] Wu S., You Y., An P., Kanno T., Nakae H. Effect of modification and ceramic particles on solidification behaviour of aluminium-matrix composites. *J. Mater. Sci.* 2002;37:1855-1860.
- [15] Quian M., Taylor J.A., Yao J.Y., Couper M.J., St John D.H. A practical method for identifying phase particles in aluminium alloys by electron probe microanalysis. *J. Light Met.* 2001;1:187-193.
- [16] Asthana R. Review Reinforced cast metals – Part I Solidification microstructure. *J. Mater. Sci.* 1998;33:1679-1698.
- [17] Wu Y., Liu H., Lavernia E.J. Solidification behaviour of Al-Si/SiC MMCs during wedge-mold casting. *Acta Metall. Mater.* 1994;42(3):825-837.
- [18] Paray F., Gruzleski J.E. Effect of modification on aluminium matrix of Al-Si-Mg alloys. *Mater. Sci. Techn.* 1994;10(9):757-761.
- [19] Conley J.G., Huang J., Asada J., Akiba K. Modelling the effects of cooling rate. Hydrogen content, grain refiner and modifier on microporosity formation in Al A356 alloys. *Mater. Sci. Engng.* 2000;A285:49-55.